Hindawi Publishing Corporation
Advances in OptoElectronics
Volume 2011, Article ID 394683, 8 pages
doi:10.1155/2011/394683

*Research Article*

# Moldless PEGDA-Based Optoelectrofluidic Platform for Microparticle Selection

**Shih-Mo Yang,[1] Tung-Ming Yu,[1] Ming-Huei Liu,[2] Long Hsu,[1] and Cheng-Hsien Liu[3]**

[1] *Department of Electrophysics, National Chiao Tung University, Hsinchu 30010, Taiwan*
[2] *R & D Division, SINONAR Corporation, Hsinchu 30078, Taiwan*
[3] *Department of Power Mechanical Engineering, National Tsing Hua University, Hsinchu 30010, Taiwan*

Correspondence should be addressed to Cheng-Hsien Liu, liuch@pme.nthu.edu.tw

Received 6 March 2011; Revised 20 May 2011; Accepted 4 June 2011

Academic Editor: Aaron T. Ohta



This paper reports on an optoelectrofluidic platform which consists of the organic photoconductive material, titanium oxide phthalocyanine (TiOPc), and the photocrosslinkable polymer, poly (ethylene glycol) diacrylate (PEGDA). TiOPc simplifies the fabrication process of the optoelectronic chip due to requiring only a single spin-coating step. PEGDA is applied to embed the moldless PEGDA-based microchannel between the top ITO glass and the bottom TiOPc substrate. A real-time control interface via a touch panel screen is utilized to select the target 15 $\mu$m polystyrene particles. When the microparticles flow to an illuminating light bar, which is oblique to the microfluidic flow path, the lateral driving force diverts the microparticles. Two light patterns, the switching oblique light bar and the optoelectronic ladder phenomenon, are designed to demonstrate the features. This work integrating the new material design, TiOPc and PEGDA, and the ability of mobile microparticle manipulation demonstrates the potential of optoelectronic approach.

## 1. Introduction

The microparticle manipulation by using either optical forces or electrokinetics has been getting important and popular, especially in fields like lab-on-a-chip. The former utilize a laser beam to trap microparticles toward the focal point. The invention of optical tweezers [1–3] and the various development of the holographic optical tweezers [4, 5] have established a convenient platform to manipulate either single or multimicroparticles. However, the requirement of high N.A. value lens in optical tweezers to perform a high focal laser beam highly reduces the working distance and constrains the application [6, 7]. The latter such as dielectrophoresis (DEP) induces microparticle polarized in a nonuniform electric field to either attract or repel toward the field maximum or minimum [8, 9]. General methods to generate nonuniform electric field are to fabricate metal electrodes on the glass substrate. The fixed metal pattern limits the flexiblity to manipulate microparticle. Recently, Chiou et al. integrated the optical flexibility and the electronic approach to present optoelectronic tweezers (OETs) [10]. Its various applications have been applied in biological field [11].

Photoconductive material is a key character of the OET. The amorphous silicon (a-Si) is usually fabricated on an ITO glass to prevent the charges [12]. While the light pattern with proper absorbing wavelength is projected onto the a-Si layer, the resistance within the illumination region is reduced and the charges transport through the a-Si layer to form a virtual electrode. Due to the flexibility of light pattern, the nonuniform electric field induced by illuminating method is able to manipulate the microparticle within the region which the light can cover. Polystyrene particles [10, 13], biological sample [10, 11, 13–15] DNA [16, 17], and other microparticles [18–21] are able to be manipulated by this optoelectronic approach.

The micromolding approach of photocrosslinkable polymers has been widely applied in cells patterning and three-dimensional artificial tissue [22–25]. The structure of photolithographically patterned poly(ethylene glycol) diacrylate (PEGDA) enables to fabricate microwell array [26, 27], cultures cells inside hydrogels [28], and forms cell-laden

microgels for the fabrication of 3D tissue constructs [29]. The high-resolution feature of photolithographically patterned PEGDA hydrogel has been also applied to photoresist-based patterns [30] as master molds for generating poly(dimethylsiloxane), PDMS, microstructures [31]. Comparing to the methods of turning the PDMS microfluidics from PEGDA-based mold, here we present the approach of fabricating the microchannel which is directly embedded into the optoelectrofluidic chip.

Polymer-based and organic material OET devices have been reported [32, 33]. Herein, we use the simplified fabrication process with the photoconductive material, titanium oxide phthalocyanine (TiOPc), to fabricate our optoelectrofluidic chip. Comparing with a-Si deposition process, a single spin-coating step is able to finish the fabrication of our TiOPc-based OET chip. We also demonstrate the PEGDA microchannel used for pumping and injecting the medium containing polystyrene particles. This integration providing a tunable and constant liquid flow velocity promotes the optoelectronic technology as a optoelectrofluidic platform for the microparticle manipulation. By utilizing dynamic optical images to generate the light-induced DEP force, this plateform demonstrates the feature of microparticle selection which can be done by the design of either the switching oblique light bar or the fixed slanting in-parallel light bars.

## 2. Principle of TiOPc-Based Light-Induced Dielectrophoresis Chip

DEP was investigated by H. A. Pohl (1951), who performed the early significant experiments with the small plastic microparticles suspended in insulating dielectric liquid and found that they could be driven in response to the application of a nonuniform electric field [34, 35]. This phenomenon has been applied to manipulate the microparticles such as virus, bacteria, neurons, and limited cells in microfluidics [36]. The time-averaged DEP force, $F_{\mathrm{DEP}}$, acting on a spherical microparticle of radius $r$ suspended in the insulating medium of relative permittivity $\varepsilon_m$ is given by

$$F_{\mathrm{DEP}} = 2\pi r^3 \varepsilon_m \,\mathrm{Re}\left[f_{\mathrm{CM}}(\omega)\right] \nabla E_{\mathrm{rms}}^2. \tag{1}$$

Here, $E_{\mathrm{rms}}^2$ is the root mean square of the ac electric field, and $f_{\mathrm{CM}}(\omega)$ is the Clausius-Mossotti factor [36, 37].

In our PEGDA-based optoelectrofluidic platform, the microparticles are suspended in the insulating medium and sandwiched between the top indium tin oxide (ITO) conductive glass and the bottom photoconductive layer substrate. The feature of photoconductivity is that its conductivity can be enhanced when the suitable wavelength light illuminates on it. In the illumination region, the charges transport the conductivity layer and assemble on its surface to form a virtual electrode. The size of virtual electrode on the photoconductivity surface is much smaller than the top ITO plane, relatively. Therefore, the electric field intensity within the illumination region is the maxima, while ac voltage is applied between the top and the bottom ITO glasses. The microparticle experiences either the positive DEP force attracting toward the light pattern or the negative DEP force repelling toward the nonilluminated region. In this paper, the microparticles, polystyrene beads, always experience the negative DEP force [13] under our operation condition setup.

## 3. Chip Fabrication

The general method to fabricate microfluidic channel takes the advantage of convenience of polydimethylsiloxane-(PDMS-) based microstructure. Utilizing standard photolithography process to fabricate SU-8 negative photoresist on the silicon substrate and turning the case mold with PDMS are widely used to form the designed microchannels. It is a convenient approach for a microchannel with any complex component. However, for our optoelectrofluidic platform with the top ITO glass and the bottom TiOPc substrate, a thin PDMS film is easy to remain on the top ITO glass above the microchannel. That would limit the electric field distribution within the microchannel.

The oxygen plasma treatment would help the bonding of the PDMS surface and the glass substrate, but the conductivity of indium oxide layer on the glass plane would reduce the bonding force between itself and PDMS surface. Therefore, PDMS microchannel is not the first choice for our light-induced dielectrophoresis chip.

This research integrates the OET system and the microchannel structure. Professor Lee's group utilizes a light bar switch to select the polystyrene beads of specific diameter into the desired channel [38]. Professor Wu's group uses the dynamic nonuniform electric field to induce the cells electroporation and get the fluorescent tags through the membrane into the cell [39]. Both of them utilize positive photoresist SU-8 to fabricate the microchannels. Besides, the latter applies the UV-curable epoxy to seal the SU8 microchannel. Although the SU-8 provides a convenient way to guide the liquid flow on a-Si-based OET chip, it is not the good choice for our organic photoconductive TiOPc-based chip. The hardened TiOPc layer would be dissolved in the alcoholic solution. Besides, the solvent to develop the SU-8 structure on TiOPc surface would also destroy the TiOPc characters. TiOPc would be washed out by these two organic solutions. Therefore, we develop the PEGDA material to fabricate the microchannel in this research. Besides, it is much convenient to fabricate PEGDA-based microchannels because there is no need to make the mold first. Moreover, there are usually three PDMS walls for the PDMS channel, two sides and one top cover. The PEGDA-based channel only has two side PEGDA walls. It keeps the features of the top ITO glass and the bottom substrates. This is suitable for our TiOPc-based optoelectronic chip.

The schematic of the process to fabricate the moldless PEGDA-based microchannel on the TiOPc-based optoelectrofluidic chip is shown in Figure 1. The TiOPc liquid is dropped on a 3 cm × 8 cm ITO glass substrate. The thin TiOPc layer of about 500 nm is spin coated at 1000 rpm for 10 sec (Figures 1(a) and 1(b)). After baking at 130°C for 30 min to remove the organic solvent and harden the photoconductivity structure, the thin TiOPc layer stays stable for

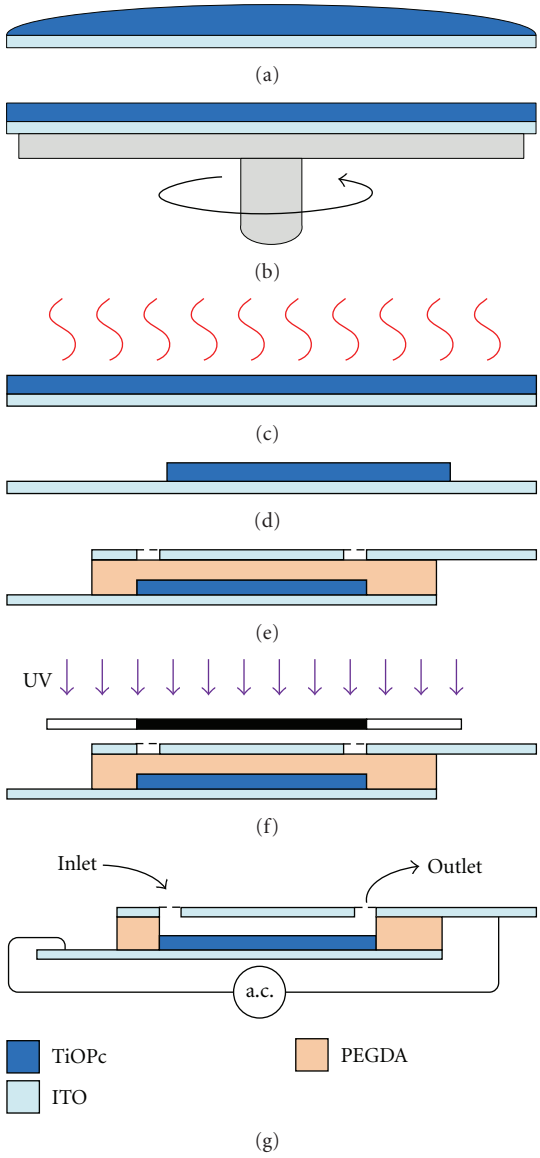


Figure 1: Fabrication process of the TiOPc-based light-induced DEP chip and the moldless PEGDA-based microchannel.

months on the ITO glass surface under normal operation (Figure 1(c)). Because our operation area is about 3 cm × 8 cm, the ethanol-water solution (70 : 30) is utilized to wipe out the unused area and remain the suitable operation area of TiOPc surface (Figure 1(d)). The PEGDA prepolymer solution, which is prepared by mixing 5 mL of PEGDA (MW 258 Da, 99%) with 150 mg of 2,2-dimethoxy-2-phenyl-acetophenone (DMPA, 99%) photoinitiator, is sandwiched between the top ITO glass and the bottom TiOPc-coated substrate (Figure 1(e)). The UV light of 350~500 nm wavelength illuminates on the chip for several seconds (Figure 1(f)). After photocrosslinking, microchannel is developed by utilizing DD-water to remove the noncrosslinked prepolymer and dried with $N_2$ blowing. Finally, the chip is placed on the hotplate at 40°C for 30 min to remove the water vapour and harden the PEGDA-based microstructure.

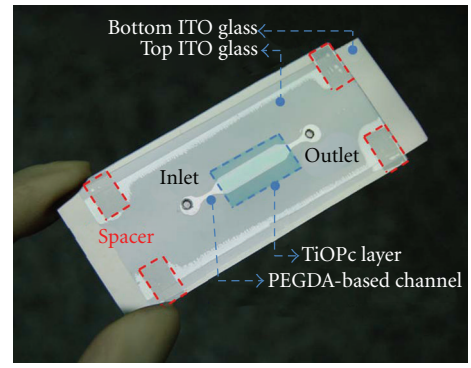


Figure 2: The moldless PEGDA-based optoelectrofluidic chip prototype. The overlapping area of TiOPc layer and PEGDA-based channel is the working region.

The moldless PEGDA-based optoelectrofluidic chip prototype is shown in Figure 2. The TiOPc layer is spincoated on the bottom ITO glass. Inlet and outlet holes are drilled on the top ITO glass. Before the UV light exposure, the four square spacers of 60 $\mu$m height are placed at the corners of the exposure region. The prepared PEGDA solution is sandwiched between bottom and top ITO glasses. After photocrosslinking of UV light illuminating, the microchannel is formed between the two ITO glasses.

## 4. The Operation System Setup for the TiOPc-Based Light-Induced Dielectrophoresis Chip

The optoelectrofluidic platform consists of three parts, the optical system, the optoelectronic chip, and the liquid pumping setup. The light source is provided by a Philips UHP mercury lamp and concentrated as a straight beam when it passes through a pair of focusing lenses, an optical alignment. The light illuminates on a digital micromirror display (DMD, with a spatial resolution of 1024 × 768 pixels). The pattern of micromirror is controlled by a touch-panel device, MSI AE 2000, and the manipulation interface is programmed by using Flash software (Adobe Systems Co., Ltd.). After the illuminating light reflects from the DMD surface, the light pattern is formed as the designed pattern on the controlled surface. A pair of focus lenses, which consist of two lenses with 200 and 10 mm focal lengths respectively, are utilized to concentrate the pattern size as 1/20 times and project the light pattern onto the TiOPc surface. The chip is placed on an XYZ translation stage for tuning the projected image. A function generator (33120A, Agilent) is used to provide the out-of-phase ac voltage required for the DEP operation on the optoelectrofluidic platforms. A syringe pump (SP230IW, WPI, Fl., USA) is utilized to pump and regulate the flow streams containing with the microparticles polystyrene beads. The motion of microparticles manipulated by light image is captured and recorded by a 10x object lens and a digital CCD camera connecting to a desktop computer (Figure 3).

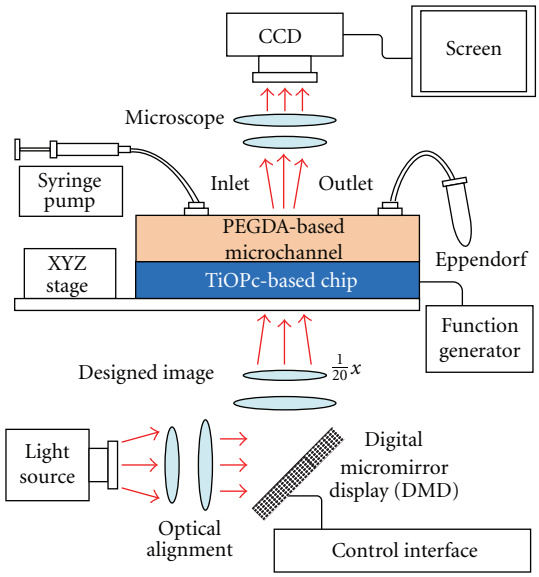


Figure 3: Schematic diagram of the optoelectrofluidic system. The optical system, the optoelectrofluidic platform, and the liquid driving pump are three main parts.

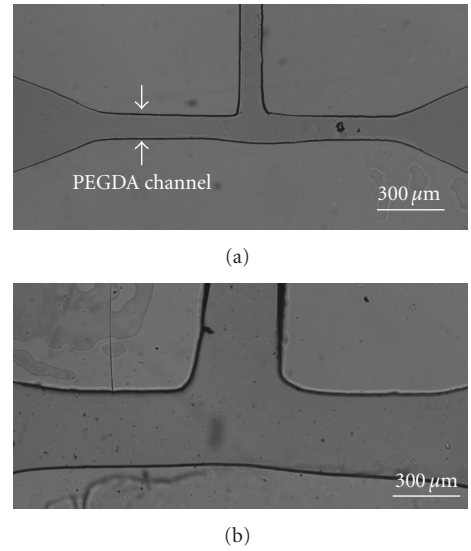


Figure 4: T junction of PEGDA-based microchannel. (a) 100 $\mu$m wide microchannel and (b) 300 $\mu$m wide microchannel.

## 5. PEG-Based Microchannel

Here, we design the T junction pattern for the PEGDA-based microchannel. The channel width in Figures 4(a) and 4(b) is 100 $\mu$m and 300 $\mu$m, respectively, for two different microchannel designs. Before UV light illuminating, the PEGDA solution of about 50 $\mu$l is sandwiched between the top and the bottom glasses. After 7 seconds of UV photopolymerization process, the microchannel is fabricated and exhibits a good optical transparency and robust package. The DMPA ratio in PEGDA solution determines the exposure time and the later microstructure expansion. The diffraction influence of UV illuminating is a significant phenomenon when the PEGDA solution is exposed. According to our experimental results, we could easily fabricate the microchannel of about 100 $\mu$m width.

## 6. Optical Virtual-Electrode Switch for Microparticle Selection

When the light pattern is projected on the photoconductivity material, the conductivity is reduced, and the charges transport to the TiOPc layer to form a virtual electrode, on its surface. Microparticles would be either attracted toward the light pattern due to the positive DEP force or repelled to the nonilluminated region due to the negative DEP force. If the microfluidics system is integrated with this DEP operation, the microparticle would experience liquid driving force dominated by the liquid flow. This integration of microfluidics and light-induced DEP increases the operation flexibility.

Here, we combine the convenience of light-driven operation with the feature of moldless PEGDA-based microfluidics channel to develop the optical virtual switch approach for microparticle selection as shown in Figure 4(a). The light pattern projected on the TiOPc surface has two different functional regions, alignment part and virtual switch part. The liquid flows rightward in the PEGDA-based microchannel containing with the dispersedly suspended microparticles. In order to arrange the microparticle as a line one by one, the light pattern with the funnel-like geometry is designed for the entrance guiding. When the microparticle reaches the edge of light pattern, it experiences a repelling force (negative DEP) toward nonilluminated region. In Figure 5(a), the direction of flow-driving force is rightward, and the direction of OET force is in the upper left. These two forces dominate the net force, $F_{\text{Net}}$, which is in the direction of the up right at the entrance of the switch. Then, the microparticle is able to be selected into the specific downstream pathway based on our virtual switch command. The upper channel and down channel are two flash models, as shown in Figures 5(c) and 5(d), to guide the microparticle into different pathway. The polystyrene bead experiences negative DEP force and only moves within the minimum electric field region which is the nonilluminated region on the TiOPc surface. To preverify the DEP effect induced by the light pattern for predicting the trajectory of moving microparticles, a commercial finite element software CFD-ACE+ (CFDRC, Huntsville, Ala) is utilized to simulate the steady-state electric field, which dominates the DEP force to drive the mobile microparticles. Figure 5(b) shows the simulation result of electric field distribution, $E$_square, on the chip. The illumination region has the large electric field, and the nonilluminated region provides the minimum electric field for polystyrene bead. The negative DEP force guides the bead at the nonilluminated region, and the liquid flow drives it to move rightward as the black-dotted line shown in Figure 5(b). This research work integrates touch panel for the convenient and intuitive microparticle manipulation. The real-time controlling interface is programmed by using Flash

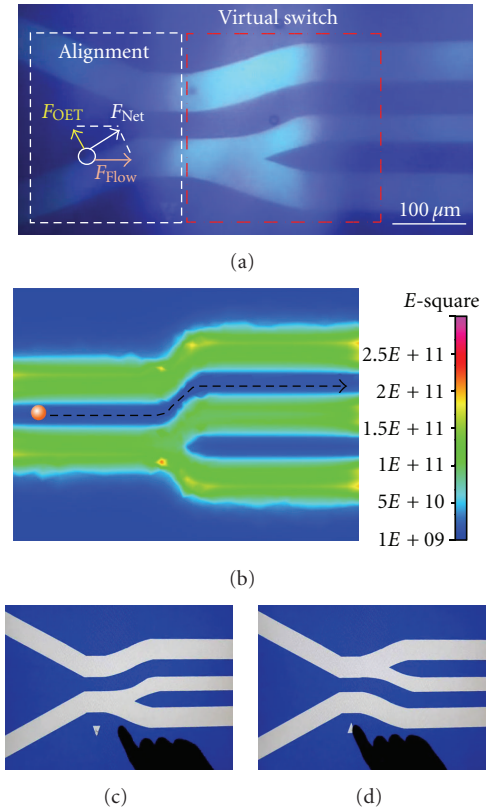


FIGURE 5: (a) Optical virtual-electrode switch. (b) Numerical simulation of the virtual-electrode switch. (c) The upperchannel model and (d) downchannel model light image on the touch panel for control interface. The black shape is the finger for triggering the model switch.

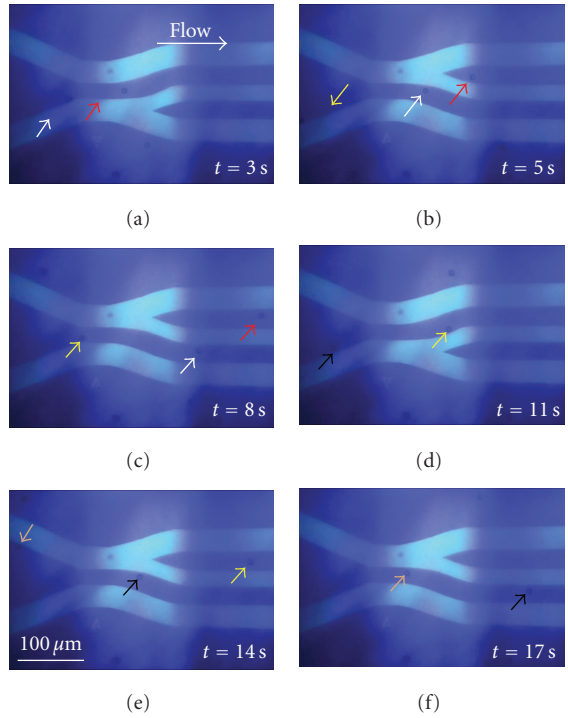


FIGURE 6: (a)–(f) The microparticle selection process. The microparticles with the velocity of 100 $\mu$m/s are selected toward different downstream channel by our designed light pattern.

software. The light pattern switch between upper-channel and down-channel models is triggered by the functional triangle image shown in Figures 5(c) and 5(d). The touch panel screen and the feature of Flash software provide a user-friendly interface. We switch the light image of different modes on the TiOPc surface by the finger shown in Figures 5(c) and 5(d). As a mobile microparticle moving from the entrance, we can select the microparticle to move in the desired downstream pathway by the simple finger operation.

The selection process of microparticles based on the optical virtual-electrode switch is demonstrated and recorded as shown in Figures 6(a)–6(f). The different color arrows/dotted circles indicate the moving path of the individual bead in the microchannel. The microparticles are arranged one by one toward the entrance by the funnel-shape light pattern, which generates negative DEP force. The microparticle enters the selection region with a characterized velocity of 100 $\mu$m/s. When the light pattern is in upper-channel model, the polystyrene bead will be guided to the upper pathway.

When the light pattern is in down-channel model, the polystyrene bead will be guided to the lower pathway. The light pattern mode is switched from the under-channel model to the down-channel mode by touching the triangle on the touch panel screen to trigger operation mode switch. Figures 6(a)–6(f) demonstrate the switch and selection process for different microparticles. The beads indicated by yellow, black, and orange colors are arranged in order to the entrance and selected to different desired channels. These processes demonstrate that utilizing light pattern projecting onto the TiOPc chip to select desired mobile polystyrene bead provides a convenient platform for microparticle selection.

## 7. Optoelectronic Ladder Effect for Microparticle Sorting

Optoelectronic ladder effect is another application utilizing the virtual electrode to sort mobile microparticles. As a line-shape light pattern projected onto the TiOPc chip surface, a virtual electrode like a line is formed on the TiOPC surface, and a nonuniform electric field is generated in space. When a moving microparticle encounters this electric field, it would experience an either attracting or repelling DEP force. The force from liquid flow, $F_{Flow}$, drives the microparticle rightward. The second force, $F_{OET}$, acting on the microparticle is provided from the nonuniform electric field with the DEP direction perpendicular to the linear light pattern. The net force, $F_{Net}$, as illustrated in Figure 6(a) drives the microparticle toward the right-up direction along the virtual electrode, the linear light bar. Because the electric field distribution of the nonuniform electric field is three dimensions as shown in Figure 7, the microparticle is elevated to stride

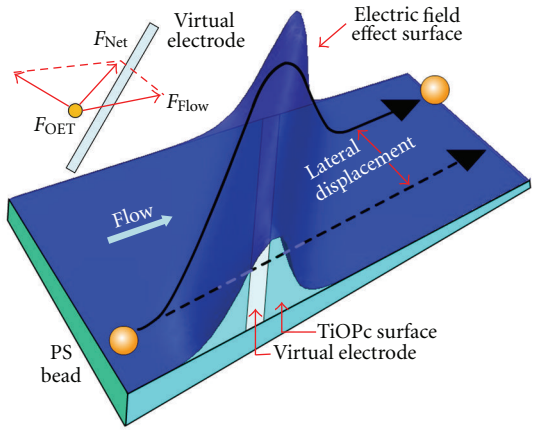


Figure 7: The simulation of nonuniform electric field distribution generated due to the linear light-induced virtual electrode pattern.

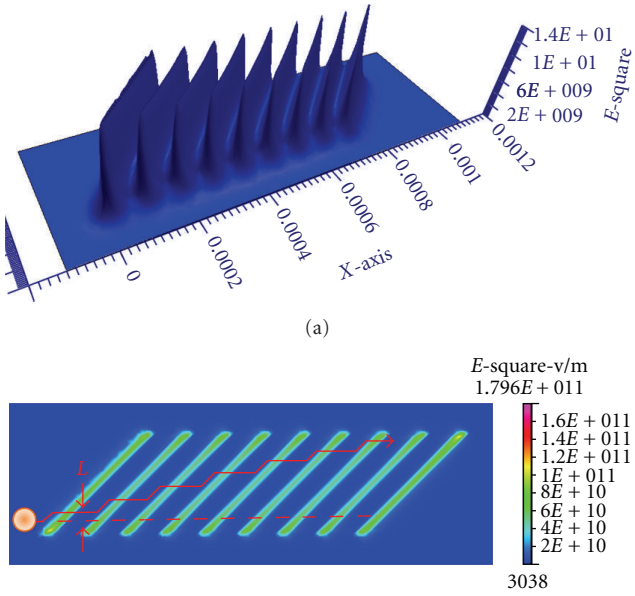


Figure 8: Electric field simulation for the optoelectronic ladder effect induced by the in-parallel slanting light bars. (a) Side view and (b) top view of the induced electric field distribution.

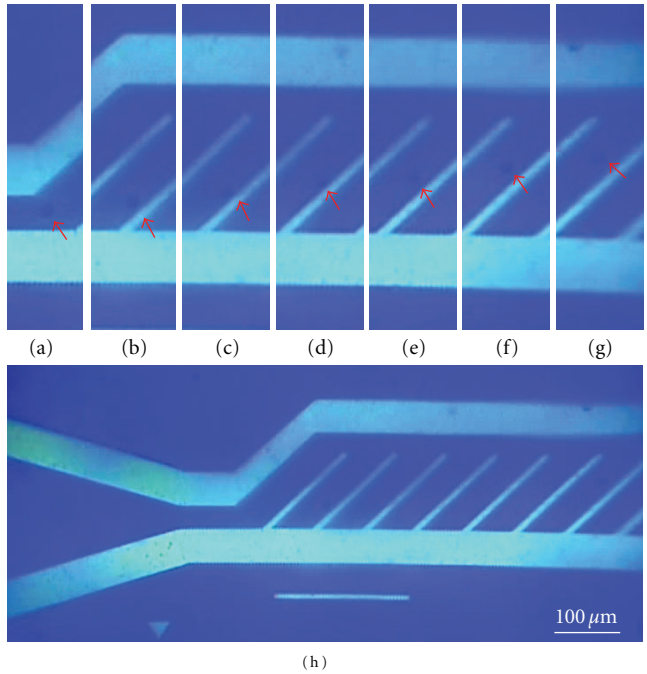


Figure 9: (a)–(g) The red arrow/dotted circle indicates the position of microparticle along the microchannel. The lateral displacement is enlarged by a series of DEP forces generated due to TiOPc-based light-induced dielectrophoresis. The time interval of each image is 0.5 sec. (h) The light image projected on the TiOPc surface.

across the virtual electrode like climbing a mountain. As it passes and falls down to the TiOPc surface and keeps moving, this process generates a lateral displacement between the original and final moving directions.

Utilizing a series of slanting linear light image to generate three-dimensional nonuniform electric field for the lateral displacement of microparticles is the concept of our optoelectronic ladder effect. When a microparticle passes one light image, the microparticle particle has a one-step lateral displacement, $L$, between the original and the final moving direction. Several slanting linear light bars in parallel would enlarge these lateral displacements. The trace of the microparticle crossing over these series of in-parallel light images is just like a ladder. Figure 8(a) shows the simulation of electric field distribution for a series of slanting light-bar pattern, which is utilized to enlarge the lateral displacement of the microparticle. Figure 8(b) illustrates the moving trajectory of the microparticle when it passes the in-parallel slanting light-bar pattern. As the flow velocities are 520 $\mu$m/s, 260 $\mu$m/s, and 150 $\mu$m/s, the average lateral displacements of microparticles crossing the slating light bar are 5.2 $\mu$m, 8.1 $\mu$m, and 11.9 $\mu$m, respectively. The distance of lateral displacement could be assigned and tuned via the flow velocity.

The experimental recording for the trajectory of the moving microparticle experiencing the nonuniform electric field is shown in Figure 9(a)–9(g). Figure 9(h) is the light pattern projected on the TiOPc surface. The front part with the shape similar to a funnel is utilized to line up the microparticles to enter the entrance. While the microparticle moving rightward encounters the slanting light-bar image, the negative DEP force would push it upward to make a lateral distance between the original and the final direction. The red arrow/dotted circle indicates the microparticle position. The more slanting light bars more the microparticle passes, the more lateral displacement would be enlarged.

The microparticle lateral displacement is dominated by the TiOPc-based light-induced DEP force and the liquid flow driving force. Therefore, the tuning of the liquid flow would also influence the lateral displacement of the microparticle. The relationship between the lateral displacement and the flow velocity is characterized and shown in Figure 10. The time of the microparticle moving from TiOPc surface to the DEP-force-constrained height in the nonuniform electric

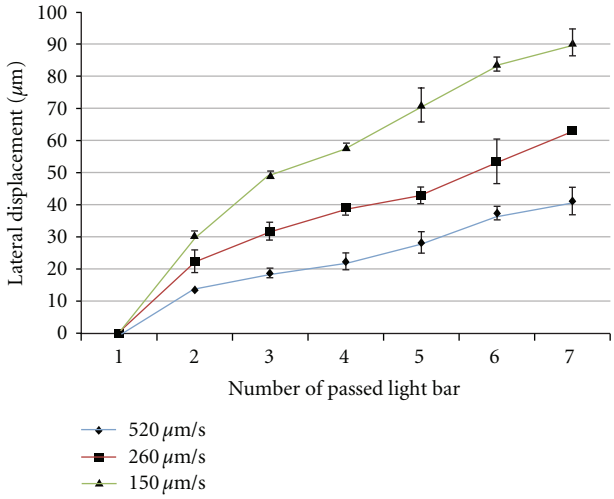


FIGURE 10: The relationship of lateral displacement in different flow velocity. The lateral displacement is enlarged in the low flow velocity.

field determines the lateral displacement. If the microparticle spends more time climbing the mountain-shape nonuniform electric field, the net force, $F_{net}$, has more time to act on it to generalize the larger lateral displacement. A mobile microparticle with the slow velocity would have a large lateral displacement. After passing seven slanting light bars, a microparticle with 520 $\mu$m/s velocity has only 40 $\mu$m lateral displacement. For a slow velocity, 150 $\mu$m/s, its lateral displacement is 90 $\mu$m.

## 8. Conclusions

We report the development of the moldless PEGDA-based optoelectrofluidic platform for the demonstration of microparticle selection. The negative DEP force is induced by the virtual electrode which is formed due to the illuminating light pattern. The application of the organic photoconductivity material, TiOPc, simplifies the chip fabrication process. PEGDA-based microchannel is embedded onto the TiOPc layer to provide the required liquid flow. The target mobile microparticle is able to be selected by the virtual switch. The different lateral displacements of a moving polystyrene particle encountering a series of slanting light bars under distinct flow velocity are measured. With this integration, this optoelectrofluidic platform provides a suitable approach to fabricate a microfluidic system on the TiOPc-based OET chip and to supply a functional manipulation of microparticle under the continuous flow.

## Acknowledgment

This research is financially sponsored by National Science Council (Grants nos. 98-2120-M-007-003 and NSC 99-2221-E-007-125-MY3). The authors extend special thanks to Professor Hwan-You Chang at Institute of Molecular Medicine, National Tsing Hua University for the biological knowledge support. They also thank Professor Ming C. Wu at University of California, Berkeley, Prof. Pei-Yu Chiou at University of California, Los Angeles, and Professor Gwo-Bin Lee at National Tsing Hua University for sharing OET experience and helpful discussion.

## References

[1] P. S. Dittrich and A. Manz, "Lab-on-a-chip: microfluidics in drug discovery ," *Nature Reviews Drug Discovery*, vol. 5, no. 3, pp. 210–218, 2006.

[2] A. Ashkin, J. M. Dziedzic, and T. Yamane, "Optical trapping and manipulation of single cells using infrared laser beams," *Nature*, vol. 330, no. 6150, pp. 769–771, 1987.

[3] K. C. Neuman and S. M. Block, "Optical trapping," *Review of Scientific Instruments*, vol. 75, no. 9, pp. 2787–2809, 2004.

[4] E. R. Dufresne and D. G. Grier, "Optical tweezer arrays and optical substrates created with diffractive optics," *Review of Scientific Instruments*, vol. 69, no. 5, pp. 1974–1977, 1998.

[5] B. Sun, Y. Roichman, and D. G. Grier, "Theory of holographic optical trapping," *Optics Express*, vol. 16, no. 20, pp. 15765–15776, 2008.

[6] J. R. Moffitt, Y. R. Chemla, S. B. Smith, and C. Bustamante, "Recent advances in optical tweezers," *Annual Review of Biochemistry*, vol. 77, no. 1, pp. 205–228, 2008.

[7] D. G. Grier, "A revolution in optical manipulation," *Nature*, vol. 424, no. 6950, pp. 810–816, 2003.

[8] R. Pethig, "Dielectrophoresis: status of the theory, technology, and applications," *Biomicrofluidics*, vol. 4, no. 2, article 022811, 35 pages, 2010.

[9] C. Zhang, K. Khoshmanesh, A. Mitchell, and K. Kalantar-Zadeh, "Dielectrophoresis for manipulation of micro/nano particles in microfluidic systems," *Analytical and Bioanalytical Chemistry*, vol. 396, no. 1, pp. 401–420, 2010.

[10] P. Y. Chiou, A. T. Ohta, and M. C. Wu, "Massively parallel manipulation of single cells and microparticles using optical images," *Nature*, vol. 436, no. 7049, pp. 370–372, 2005.

[11] Y. S. Lu, Y. P. Huang, J. A. Yeh, C. Lee, and Y. H. Chang, "Controllability of non-contact cell manipulation by image dielectrophoresis (iDEP)," *Optical and Quantum Electronics*, vol. 37, no. 13–15, pp. 1385–1395, 2005.

[12] H.-Y. Hsu, A. T. Ohta, P. Y. Chiou, A. Jamshidi, S. L. Neale, and M. C. Wu, "Phototransistor-based optoelectronic tweezers for dynamic cell manipulation in cell culture media," *Lab on a Chip*, vol. 10, no. 2, pp. 165–172, 2010.

[13] A. T. Ohta, P. Y. Chiou, T. H. Han et al., "Dynamic cell and microparticle control via optoelectronic tweezers," *Journal of Microelectromechanical Systems*, vol. 16, no. 3, pp. 491–499, 2007.

[14] A. T. Ohta, P. Y. Chiou, H. L. Phan et al., "Optically controlled cell discrimination and trapping using optoelectronic tweezers," *IEEE Journal on Selected Topics in Quantum Electronics*, vol. 13, no. 2, pp. 235–242, 2007.

[15] A. T. Ohta, M. Garcia, J. K. Valley et al., "Motile and non-motile sperm diagnostic manipulation using optoelectronic tweezers," *Lab on a Chip*, vol. 10, no. 23, pp. 3213–3217, 2010.

[16] M. Hoeb, J. O. Rädler, S. Klein, M. Stutzmann, and M. S. Brandt, "Light-induced dielectrophoretic manipulation of DNA," *Biophysical Journal*, vol. 93, no. 3, pp. 1032–1038, 2007.

[17] P.-Y. Chiou, A. T. Ohta, A. Jamshidi, H. Y. Hsu, and M. C. Wu, "Light-actuated AC electroosmosis for nanoparticle manipulation," *Journal of Microelectromechanical Systems*, vol. 17, no. 3, pp. 525–531, 2008.

[18] A. Jamshidi, P. J. Pauzauskie, P. J. Schuck et al., "Dynamic manipulation and separation of individual semiconducting and metallic nanowires," *Nature Photonics*, vol. 2, no. 2, pp. 86–89, 2008.

[19] A. T. Ohta et al., "Trapping and transport of silicon nanowires using lateral-field optoelectronic tweezers," in *Proceedings of the Conference on Lasers and Electro-Optics (CLEO '07)*, 2007.

[20] A. T. Ohta, S. L. Neale, H. Y. Hsu, J. K. Valley, and M. C. Wu, "Parallel assembly of nanowires using lateral-field optoelectronic tweezers," in *Proceedings of the 2008 IEEE/LEOS International Conference on Optical MEMS and Nanophotonics (OPT MEMS '10)*, pp. 7–8, August 2008.

[21] M.-C. Tien, A. T. Ohta, K. Yu, S. L. Neale, and M. C. Wu, "Heterogeneous integration of InGaAsP microdisk laser on a silicon platform using optofluidic assembly," *Applied Physics A*, vol. 95, no. 4, pp. 967–972, 2009.

[22] A. Khademhosseini, G. Eng, J. Yeh et al., "Micromolding of photocrosslinkable hyaluronic acid for cell encapsulation and entrapment," *Journal of Biomedical Materials Research*, vol. 79, no. 3, pp. 522–532, 2006.

[23] D. T. Chiu, N. L. Jeon, S. Huang et al., "Patterned deposition of cells and proteins onto surfaces by using three-dimensional microfluidic systems," *Proceedings of the National Academy of Sciences of the United States of America*, vol. 97, no. 6, pp. 2408–2413, 2000.

[24] J. Fukuda, A. Khademhosseini, Y. Yeo et al., "Micromolding of photocrosslinkable chitosan hydrogel for spheroid microarray and co-cultures," *Biomaterials*, vol. 27, no. 30, pp. 5259–5267, 2006.

[25] J. W. Nichol, S. T. Koshy, H. Bae, C. M. Hwang, S. Yamanlar, and A. Khademhosseini, "Cell-laden microengineered gelatin methacrylate hydrogels," *Biomaterials*, vol. 31, no. 21, pp. 5536–5544, 2010.

[26] Y. S. Hwang, G. C. Bong, D. Ortmann, N. Hattori, H. C. Moeller, and A. Khademhosseinia, "Microwell-mediated control of embryoid body size regulates embryonic stem cell fate via differential expression of WNT5a and WNT11," *Proceedings of the National Academy of Sciences of the United States of America*, vol. 106, no. 40, pp. 16978–16983, 2009.

[27] H. C. Moeller, M. K. Mian, S. Shrivastava, B. G. Chung, and A. Khademhosseini, "A microwell array system for stem cell culture," *Biomaterials*, vol. 29, no. 6, pp. 752–763, 2008.

[28] J. A. Burdick and K. S. Anseth, "Photoencapsulation of osteoblasts in injectable RGD-modified PEG hydrogels for bone tissue engineering," *Biomaterials*, vol. 23, no. 22, pp. 4315–4323, 2002.

[29] Y. Du, E. Lo, S. Ali, and A. Khademhosseini, "Directed assembly of cell-laden microgels for fabrication of 3D tissue constructs," *Proceedings of the National Academy of Sciences of the United States of America*, vol. 105, no. 28, pp. 9522–9527, 2008.

[30] A. Revzin, R. J. Russell, V. K. Yadavalli et al., "Fabrication of poly(ethylene glycol) hydrogel microstructures using photolithography," *Langmuir*, vol. 17, no. 18, pp. 5440–5447, 2001.

[31] C. M. Hwang, W. Y. Sim, S. H. Lee et al., "Benchtop fabrication of PDMS microstructures by an unconventional photolithographic method," *Biofabrication*, vol. 2, no. 4, Article ID 045001, 2010.

[32] G.-B. Lee, Y. H. Lin, W. Y. Lin, W. Wang, and T. F. Guo, "Optically-induced dielectrophoresis using polymer materials for biomedical applications," in *Proceedings of the The 15th International Conference on Solid-State Sensors, Actuators and Microsystems (TRANSDUCERS '09)*, pp. 2135–2138, June 2009.

[33] S. M. Yang, T. M. Yu, H. P. Huang, M. Y. Ku, L. Hsu, and C. H. Liu, "Dynamic manipulation and patterning of microparticles and cells by using TiOPc-based optoelectronic dielectrophoresis," *Optics Letters*, vol. 35, no. 12, pp. 1959–1961, 2010.

[34] R. Pethig, "Dielectrophoresis: using inhomogeneous AC electrical fields to separate and manipulate cells," *Critical Reviews in Biotechnology*, vol. 16, no. 4, pp. 331–348, 1996.

[35] T. B. Jones, "Basic theory of dielectrophoresis and electrorotation," *IEEE Engineering in Medicine and Biology Magazine*, vol. 22, no. 6, pp. 33–42, 2003.

[36] C.-T. Ho, R. Z. Lin, W. Y. Chang, H. Y. Chang, and C. H. Liu, "Rapid heterogeneous liver-cell on-chip patterning via the enhanced field-induced dielectrophoresis trap," *Lab on a Chip*, vol. 6, no. 6, pp. 724–734, 2006.

[37] B. H. Lapizco-Encinas and M. Rito-Palomares, "Dielectrophoresis for the manipulation of nanobioparticles," *Electrophoresis*, vol. 28, no. 24, pp. 4521–4538, 2007.

[38] Y.-H. Lin and G.-B. Lee, "Optically induced flow cytometry for continuous microparticle counting and sorting," *Biosensors and Bioelectronics*, vol. 24, no. 4, pp. 572–578, 2008.

[39] J. K. Valley, S. Neale, H. Y. Hsu, A. T. Ohta, A. Jamshidi, and M. C. Wu, "Parallel single-cell light-induced electroporation and dielectrophoretic manipulation," *Lab on a Chip*, vol. 9, no. 12, pp. 1714–1720, 2009.